

## CHAPTER II REMOTE SENSING

### II. 1. Introduction

Remote sensing can be defined as collecting and interpreting information about an object, without being in physical contact with this object (Sabins, 1997), through the link of electromagnetic energy (Hunt, 1980). Landgrebe, (1978) defined the remote sensing as “the science of deriving information about an object from measurements made at a distance from the object”, i.e., it means obtaining information about an object without touching the object itself (Gupta, 1991).

Therefore, the term remote sensing is practically used to mean data acquisition of electromagnetic radiation (reflectance or emittance) from sensors on board of an aerial or space platform, as well as the interpretation of acquired data for deciphering ground object characteristics. This electromagnetic spectrum commonly ranges from gamma-rays to microwave radiation (Drury, 1993).

The main basic principle of remote sensing methods is that each object reflects or emits a certain intensity of light in various wavelength ranges of the electromagnetic spectrum; this is dependent upon the physical and/or the compositional characters of the object. This reflected or emitted radiation represents the spectral fingerprint or what so called the spectral signature of the corresponding object. Thus, by using the spectral curves information, it can differentiate between different types of objects. This is the basis for discrimination of various objects from their spectral behavior (Gupta, 1991; List, 1992-a).

Accordingly, remote sensing data represent a quantitative measurement of physical parameters like emitted or reflected electromagnetic radiation (EMR). The EMR constitutes the communication link between object and sensor (Hunt, 1980). Therefore, the definition of (EMR) in remote sensing is “the transported energy that can be measured and provide information on the nature of the radiating object” (List, 1992-a).

The wavelengths of EMR extended from high-energy gamma rays (<0.001 nm) to very low-frequency radio waves (>100 m). The energy of EMR photon energy is directly proportional to frequency of EMR i.e. greater energy with higher frequency and shorter wavelength (Drury, 1993).

The type of the reflected radiation at the earth’s surface is depending on its smoothness. Three types of reflection are known: specular’s reflection, which occurs when the surface is very smooth and the incident radiation is reflected back at the same angle of incident (e.g. undisturbed water surfaces, and smooth vegetation). Diffuse reflection occurs on the rough surfaces, where the radiation is equally scattered in all directions. In nature, a combination of reflection models is realized. Rocks and soils tend more to an equally distributed backscatter (List, 1992-a).

## **II. 2. The Landsat System**

Landsat was launched by NASA as the first unmanned orbital imaging satellite system of the program to investigate remote sensing of the Earth surface from space. Consequently it has been the workhorse image data acquisition system for remote sensing purposes (Richards, 1995).

Three Landsat's Imaging Systems have been used with the Landsat satellites. These are the Return Beam Vidicon (RBV), the Multispectral Scanner (MSS) and the Thematic Mapper (TM). The RBV and MSS imaging systems (sensors) were carried by Landsat-1 to Landsat-3, while; the TM sensor was carried on Landsat-4 and Landsat-5. The MSS image data are still used in geology to some extent based on their four- MSS spectral bands.

The Thematic Mapper (TM) sensor in Landsat-4 and -5 records seven (7) spectral bands with a higher spatial resolution and considered the best type of space-acquired data for geological and structural investigations. This because the TM, featuring 7 spectral bands, in comparison to the MSS 4 bands, there are an additional bands as TM-1 in the blue region makes it possible to produce natural-color images (TM 1, 2, and 3). Also two more bands, band 5 and 7, record in the short-wave infrared (SWIR). This spectral region is very important for the discrimination of OH-bearing minerals (clay minerals and soil types) and for detection of hydrothermal altered rocks. Initially the US National Aeronautics and Space Administration (NASA) developed Landsat program as experiments program. In 1983 responsibility for operating the system transferred to the National Oceanic and Atmospheric Administration (NOAA). At present (Since January 1985) the Landsat operation responsibility transferred to a private company EOSAT Inc. (Sabins, 1987; Drury, 1993).

The recent ETM+ sensor on Landsat 7 has a number of enhanced features, including: 1) New panchromatic band with 15 meters spatial resolution, co-registered with the multi-spectral bands. 2) Thermal infra-red band 6 has increased resolution from 120m to 60m, and has two gain

settings (High gain and Low gain). 3) Worldwide data - the solid state tape recorder can collect 100 images per day from anywhere in the world.

### **II. 3. Landsat Data Acquisition Index**

On the bases of the path row coordinate system, Earth Resources Observation Systems (EROS) data center archived all the Landsat satellite images (scenes) in a global indexing and referencing system named Landsat Worldwide Reference System (WRS). Accordingly, the (WRS) consists of a global network of 251 paths and 119 rows for Landsat-1 to 3 or 233 paths and 119 rows for Landsat-4 and -5.

Figure (3) illustrates the Path/Row index map of Egypt extracted from sheet 11 (GNC 11 N) of the USGS/NOAA sheets of the WRS. It shows the national center points for the Landsat-4 and 5 scenes which covering Egypt. In this index maps, the orbit paths are numbered westward, whereas the image rows are numbered southward in increasing numbers.

The path and row intersections correspond to geographic locations over which Landsat scenes are generally centered. These locations are identified by three digit path and row numbers, and when combined identify a nominal scene center.

The WRS path/row coordinates, which used to identify the Landsat-1 to 3 (MSS) and Landsat-4 and 5 (TM) scene covering the same nominal area, are vary due to the difference in their orbital characteristics.

The study area is located in the northern part of the Eastern Desert of Egypt and is covered by one scene of Landsat (ETM+), Path 176, Row 39, and date 2003.

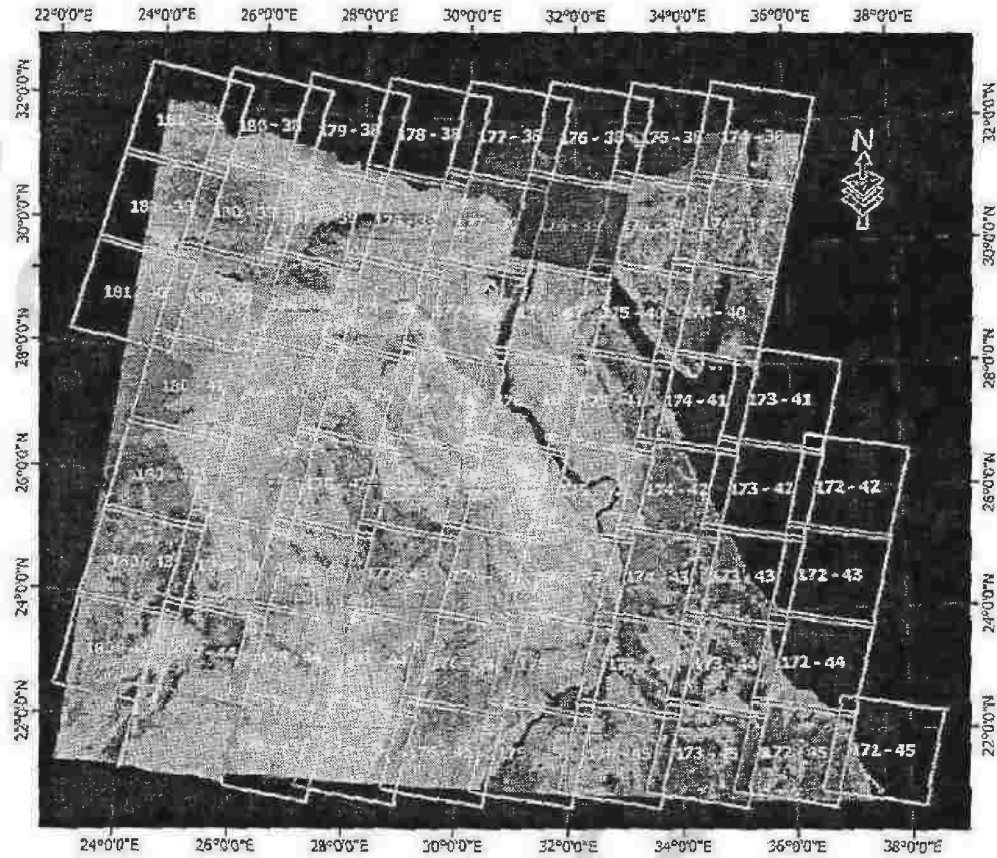


Figure (3): The Path/Row index map of Egypt extracted from the WRS sheets for the Landsat ETM+ data.

## **II. 4 Digital Image Processing and Their Interpretations**

### **II. 4. 1. Digital data preparation**

In this part, Landsat ETM+ data have been prepared for processing by making radiometric and geometric corrections to the target area. This target area is included in the scene. A subset of the target area from the scene has been applied using ERDAS Imagine 9.1 software.

### **II. 4. 2. Radiometric correction**

Radiometric corrections have been done including atmospheric haze correction. Atmospheric conditions affect of the radiance over a given object measured by the satellite sensor. The atmosphere affects the radiance measured at any point in the scene by adding a scattered radiance, termed path radiance, to the signal detected by the sensor (Kiefer and Lillesand, 1987). Thus, the radiance observed at any pixel location can be expressed by the sum of the radiance of the target plus the path radiance. This last radiance contains no valid information about ground reflectance.

The path radiance introduces a haze effect on the imagery and consequently reduces image contrast. Haze compensation procedures are designed to minimize the influence of path radiance effects. The simplest means of haze compensation in multispectral data is to assume that target area of zero reflectance must be in each band of imagery. On the bases of this assumption, the minimum pixel value for any band represents the path radiance and can be subtracted from all the pixel values in that band. This correction routine is applied uniformly throughout the image.

This is valid only if the atmospheric conditions are uniform over the scene. The haze correction of the Landsat image (for the 7 bands) was done using ERDAS Imagine 9.1 software.

### **II. 4. 3. Geometric correction (image rectification)**

In the geometric correction (image rectification), the image is rectified to match a specific map format (Topo-sheet) by assigning map coordinates to the image data (i.e. georeferencing the image data). Random geometric distribution are often corrected by analyzing well-distributed Ground Control Points (GCPs) whose locations are accurately known in the map and also occur in the image to be rectified (List, 1993).

The Landsat ETM+ image covering the area of study were georeferenced at the initial stage of this work to ease registration of the different data sets at any stage of the study and to obtain the correct geometric positions of the ground objects. To rectify the Landsat ETM+ image, about 20 GCPs were selected and encoded from the topographic maps with a scale 1:50 000 obtained from the Egyptian General Survey. However, the GCPs can also be obtained from the Global Positioning System (GPS). The selected GCPs are easily identified in both image and topographic maps. The image was georeferenced to UTM coordinate system based on a datum and spheroid of WGS84.

Finally, the generated transformation matrix was used for resampling of the pixels by employing the nearest neighbor method. The nearest neighbor approach uses the value of the closest input pixel for the output pixel value. The pixel value occupying the closest image file coordinate to the estimated coordinate will be used for the output pixel

value in the georeferenced image (Fig. 4). Through this resampling technique, all the pixels will obtain new map coordinates, and new grey value (digital number) to create new file values for the rectified image, (Lillesand and Kiefer, 1994). The pixel size has been kept at 30 m in order not to lose the spatial resolution of the Landsat TM data.

## **II. 5. Analysis of ETM+ Data**

Landsat ETM+ data is the most suitable of the present space borne sensors for geological mapping, with seven reflected spectral bands of information, there are number of image processing techniques that can be used to highlight lithology and coarse mineralogy. Landsat ETM+ data for the study area was processed for geological and structural mapping using the ERDAS Imagine 9.1.

One scene (Landsat ETM+ data) covering the investigated area, has been geometrically corrected and radiometrically balanced. Digital processing of Landsat ETM+ image for the study area, generated several products which are: single-band images interpretation, band selection and false color composite images production (bands 7, 4, 2 in Red, Green, Blue) respectively, principal component analysis (PC1, PC2, PC3, in R,B,G), and ratio images (5/7, 5/4, 3/1), (5/7, 3/1, 4/3) and (5/7, 5/1, 4) in (RGB).

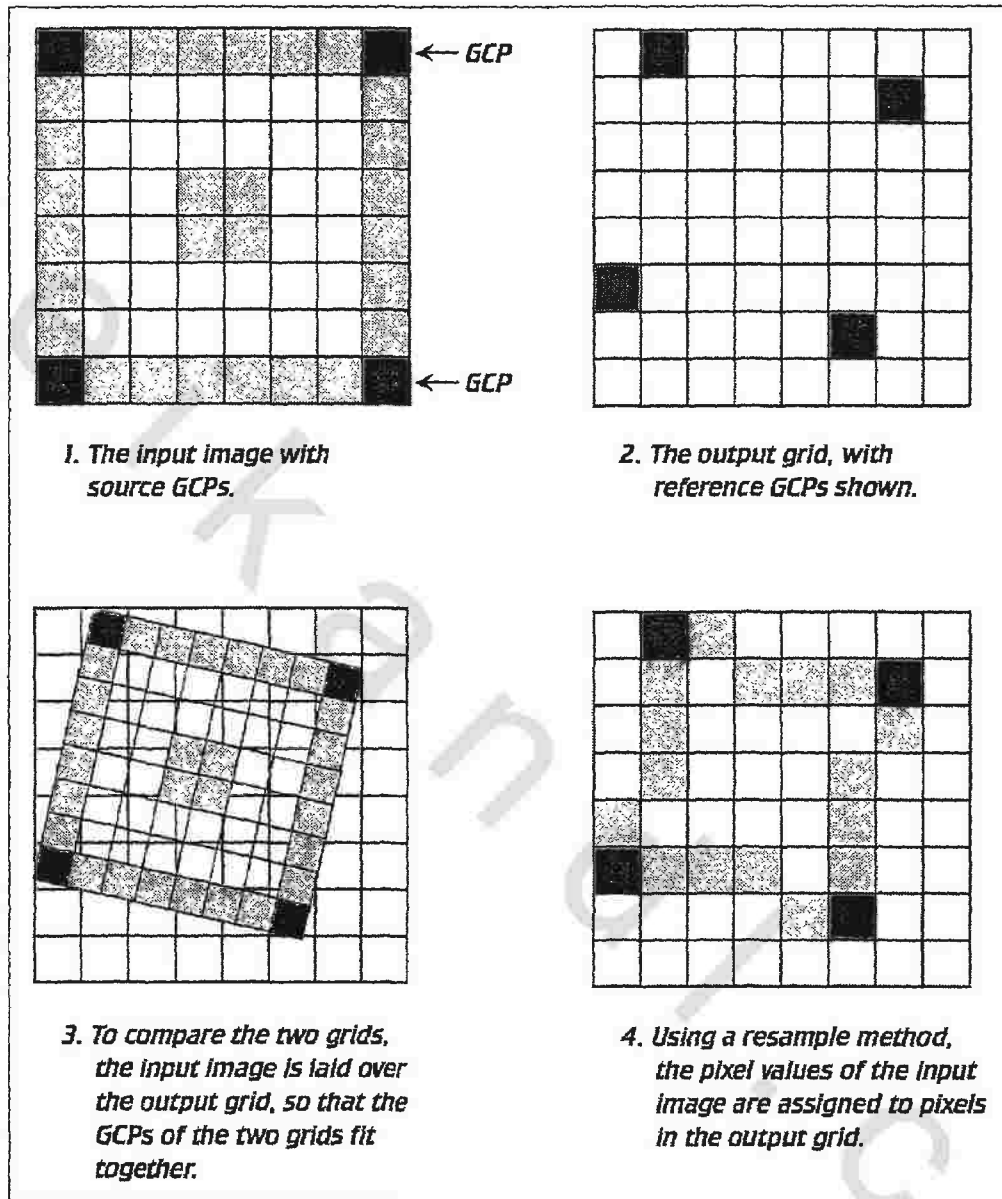


Figure (4): A diagram showing the nearest neighbor geometric correction method.

### **II. 5. 1. Single-Band Images and Their Interpretation**

Each band of the Landsat TM bands has its own characteristics and principle applications (Table 1). Single-band images for all bands are produced to notice the ability of each band in discriminating the different geological units and structures. In the present study, the TM bands of the Landsat sub-scene covering the study area were individually displayed. Band 1 is the most suitable one for the interpretation of the drainage network and the lineaments.

Bands 5 and 7 are good for the discrimination of the recent sediments from the basement rocks. The last band is band 6 that lies in the thermal region of the IR and it could be useful in determine the active faults in the study area.

### **II. 5. 2. Spectral reflectivity of rocks**

Every natural and synthetic object on the earth surfaces and near surface reflects and emits EMR over a range of wavelength in its own characteristic way according to its chemical composition and physical state. Remote sensing depends upon operation in wavelength regions where detectable differences in reflected and emitted radiation occur. Feature and their different conditions show enough variation to allow for individual identification.

In the geological interpretation of Landsat image, the spectral reflectivity of rock is often the most useful for lithologic discrimination. Spectral reflectance is a measure of amount of light reflected by material, and is expressed in images by photographic tone or color. For a multi spectral image, the spectral response is represented by the discrete digital number (DN), while the wavelength is indicated by

the band number. Therefore, the spectral signature curves can be simply constructed by plotting the image pixel value of a certain type of terrain feature as the function of band number, (Rowan and Vincent, 1971).

Plotting the spectral reflectance curves in the graphic format will allow us to determine which bands are most useful for discriminating certain type of features. The diagram below illustrates the spectral signatures for some common cover types in the study area.

By comparing the reflectance curves that obtained from the ETM+ image, (Fig. 5) it can be found that; the Miocene, the Eocene and Quaternary deposits have a high reflectance in band 4 and low reflectance with band 1, the basalt of Oligocene have a high reflectance in band 4, 5 and low reflectance with band 2 the Carboniferous rocks have a high reflectance in band 4, 5 and low reflectance with band 1.

Chapter 2  
Remote sensing

Table (1): Characteristics of the landsat TM spectral bands and their principal applications. (After Sabins, 1997).

Band	Wavelength	Characteristics and principal applications
TM-1	0.45 - 0.52	Blue-green, no MSS equivalent. Maximum penetration of water, which is useful for bathymetric mapping in shallow water (coastal studies). Useful for distinguishing soil from vegetation and deciduous from coniferous plants and cultural feature identification.
TM-2	0.52 - 0.60	Green, coincident with MSS band 4. Matches green reflectance peak of vegetation, which is useful for assessing plant vigor.
TM-3	0.63 - 0.69	Red, coincident with MSS band 5. Matches a chlorophyll absorption band that is important for discriminating vegetation types.
TM-4	0.76 - 0.90	Reflected IR, coincidence with portions of MSS bands 6 and 7. Useful for determining biomass content, vegetation types and vigor and for mapping shorelines.
TM-5	1.55 - 1.75	Reflected IR. Indicates moisture content of soil and vegetation. Penetrates thin cloud and used to discriminate it from snow. Provides good contrast between vegetation types.
TM-6	10.4 - 12.50	Thermal IR. Nighttime images are useful for thermal mapping, vegetation stress analyses and estimating soil moisture.
TM-7	2.06 - 2.35	Reflected IR. Useful for discrimination of minerals and rocks (coincides with absorption band caused by hydroxyl ions in minerals). Ratios of bands 5 and 7 are used to map Hydrothermaly altered rocks associated with mineral deposits.

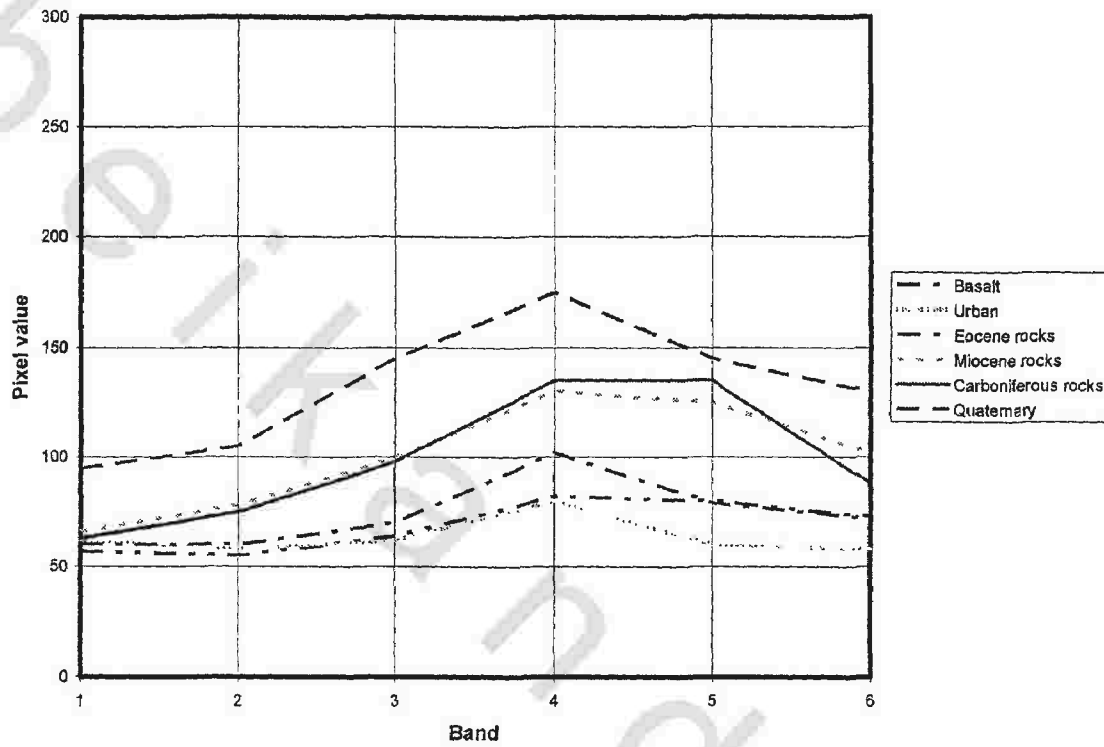


Figure (5): The spectral reflectance curves for some common rock types cover the study area.

### II. 5. 3. ETM+ band selection

A particular aspect of remote sensing is that: it provides data in multiple spectral bands (Gupta, 1991). The Landsat-5 with its seven TM bands contains a wide range of spectrally diverse data. To display a color image only three bands are required in a band combination, each directed to one of the color-guns (red, green and blue). The best band combinations are that enhance a desired target and include the most informative bands with less redundancy of information contained in these bands. The most informative band combination is that has less inter-correlated bands.

Several methods have been used for determination of the less correlated bands, and therefore to detect the best band-triplet combination. These methods are mainly based on statistical analysis of standard deviation and correlation coefficient of the TM-bands, as well as, visual inspections of the scatterograms (Feature Space Images) and the displayed colored images of various band-triplets (Fig.6).

The scatterogram or the feature space is a diagram in which two sets of image data are statistically represented through a two-dimensional plot. The location of any pixel in this diagram (space) is controlled by the DN-values of this pixel in the two plotted bands (features). The visual inspection of such a scatterogram is itself being quite informative about the mutual relation of the two bands. If the two bands are highly correlated, the scatterogram is approximated by a line, whereas, the two non-correlated bands produce a scatterogram plot in which points are scattered isotropically (Gupta, 1991).

Generally, the scatterograms for different pairs of the used TM bands were plotted and visually inspected to detect

the less correlated bands that should be use in the band-triplet (Fig. 6). The used Landsat ETM+ spectral data provide bands that are in general more or less correlated.

This is expressed by the pronounced elongated shape (more correlated) or shorted and large shape (less-correlated) of points in the scatterogram. The ranks ordering of the less correlated (i.e. more- informative) bands that concluded from visual inspection of scatterograms are shown in Table (2).

Visual inspections of the various band-triplets obtained for TM data have been carried out in order to support the statistical methods, by assigning the colors red (R), green (G), and blue (B) to bands with the order of decreasing variance Sheffield, (1985). Geological information is generally well contained in many of the high-ranking band combinations. However, the hue contrast between the different lithologic units is apparently enhanced in band-triplet 7 4 2, 5 4 1, 7 4 1, 7 5 1, 7 5 3, and 5 3 1 (as RGB) in the decreasing order. The ranking order of band composites that resulted from the methods given by Crippen (1989), and Liu and Moore (1990) are apparently nearly revealing the perfect conformity with the visual inspections. Therefore, the first band composite (7 4 2 in R G B) has been selected as the best band-triplet for the further required image processing techniques.

Table (2) shows that, no exact corroboration between the different statistical methods exemplified in selecting a particular band-triplet for Landsat TM data.

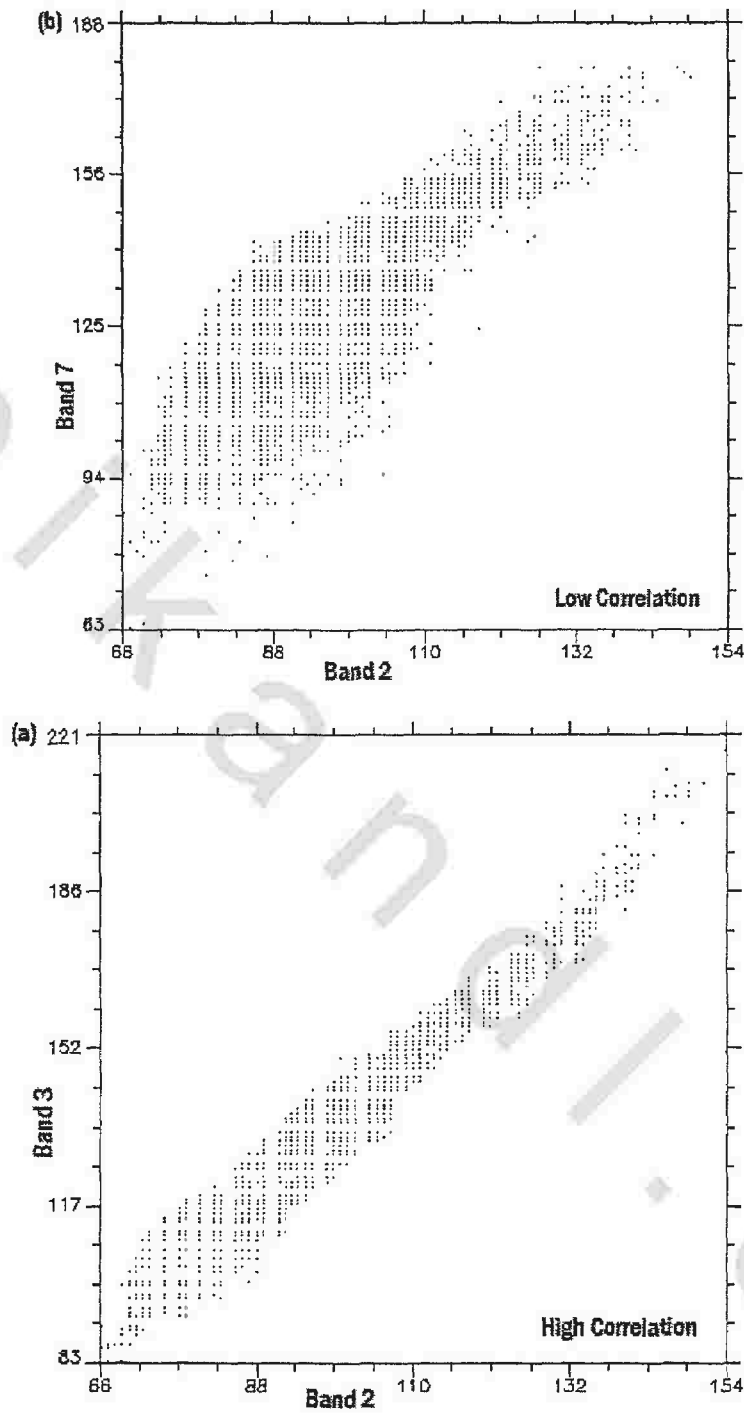


Figure (6): Scattrograms (from the study area) showing amount of correlation between different bands; (a) Highly correlated bands and (b) Low correlated bands.

Table (2) : Results of different statistical and visual inspection methods for best band-triplet selection applied to the Landsat-7 TM reflective bands covering the study area.

Method	Statistical method (R.G.B) Band-triplet				Visual inspections (R.G.B) Band-triplet	
	OIF Chavez et. Al., 1982	Determinate Sheffield, 1985	CI Crippen, 1989	IOBS Liu & McM Moor, 1990	Scatterogram	Color composite imaes
1	7,5,3	5,4,1	7,4,1	7,4,1	7,5,1	7,4,1
2	7,5,1	7,5,1	5,4,1	5,4,1	7,4,1	7,4,2
3	7,5,4	7,4,1	7,4,2	7,4,2	7,4,2	5,4,1
4	5,3,1	7,5,3	7,3,1	7,3,1	7,5,2	7,5,1
5	7,4,1	5,3,1	7,5,1	7,5,1	5,3,1	7,5,3
6	5,4,3	7,3,1	5,3,1	5,3,1	7,3,1	7,3,1
7	5,4,1	7,5,4	5,4,2	7,2,1	7,5,3	5,3,1
8	7,5,2	5,4,3	7,5,3	7,5,2	7,3,1	
9	5,4,2	7,5,2	7,2,1	5,4,2	5,4,1	
10	5,3,2	7,4,2	7,4,3	7,4,3		
11	7,3,1	5,4,2	7,5,2	7,5,4		
12	5,2,1	7,4,3	7,5,4	7,5,3		
13	7,4,2	5,2,1	5,2,1	5,2,1		
14	7,4,3	5,3,2	5,4,3	5,4,3		
15	7,3,2	7,2,1	7,3,2	7,3,2		
16	7,2,1	7,3,2	4,2,1	5,3,2		
17	4,3,1	4,3,1	4,3,1	4,2,1		
18	4,3,2	4,2,1	5,3,2	4,3,1		
19	4,2,1	4,3,2	3,2,1	3,2,1		
20	3,2,1	3,2,1	4,3,2	4,3,2		

However, the results obtained by methods of (Crippen 1989) and (Liu and Moore 1990) show significant agreement and harmony with the visual inspection.

For the other two methods, triplets containing band 5 and/or 7 tend to rank high for their high variance. In general, band combinations involving only the visible part of the electromagnetic spectrum (bands 1-3) appear to rank consistently low in all the methods because of their very high correlation coefficient, and/or low variance (Crippen, 1989). It may be summarized that in all the approaches, band-triplets constituted by each band from the visible (VIS), near infrared (IR), and middle infrared (MIR) regions apparently rank high. Band TM-5 shows the least correlated band with most of the other TM bands in their triplets.

#### **II. 5. 4. False Color Composite**

False color composite images (bands 7, 4, 2) should fair to good contrast between the Tertiary basalts and the sedimentary rocks (Fig. 7). The near infrared bands 7 and 3 indicate high reflectance in the iron zones and also indicate low reflectance in band 1. Typically, the more iron rich rocks are slightly brownish. Thus the Tertiary basalts are indicated by dark brown color, the limestone beds are whitish brownish, the wadi deposits are whitish to whitish blue color. The man made areas are dark blue color.

From these studies, it is found that the false color composite Landsat ETM+ images (7, 4, 2 in RGB) are suitable for regional tectonic structure and provide an excellent base map in which rock units are easily discriminated and geologic structures (mainly faults) are highly inferred. Also they show brightness and fair drainage pattern.

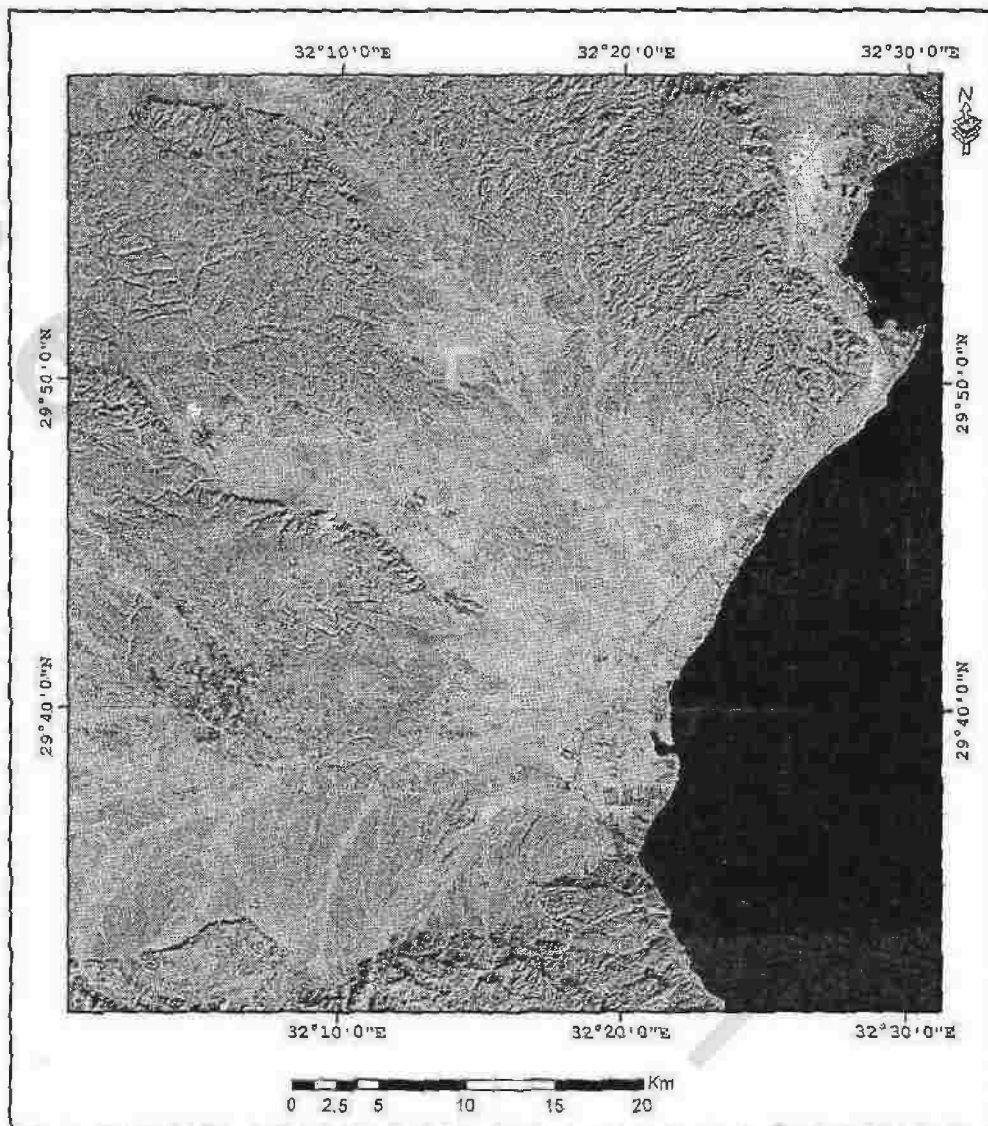


Figure (7): False color composite Landsat ETM+ image (7, 4, 2) in RGB, of the study area.

### II. 5. 5. Color Ratio Composites

A simple way of trying to extract useful information from ETM+ imagery is to perform band rationing. Band ratios describe the color of an object, although this color only corresponds to human perception when the three visible bands are considered. Ratio images are prepared by dividing the DN (digital number) in one band by the corresponding DN in another band for each pixel, stretching the resulting value, and plotting the new value as an image (Sabins, 1997).

Rationing is an effective method for distinguishing among rock types because the main spectral differences in the visible and near-infrared spectral regions are found in the slopes of the reflectivity curves.

Absorption bands are broad and weak and are difficult to use for discrimination of rock types on standard MSS images. In addition, the rationing process removes first-order brightness effects due to topographic slopes and enhances subtle color variations between materials. (Abrams et al. 1984).

For mineral mapping, the following three ratios are most widely used:

1- Band 3 / Band 1: The Fe-O charge transfer transition is characterized by a broad absorption at wavelengths less than 0.55  $\mu\text{m}$ . It is responsible for the strong red color in rocks rich in iron oxides and hydroxides. This band ratio essentially highlights red, and thus potentially iron weathered lithologies (Fig. 8).

2- Band 5 / Band 4: Iron also produces an absorption band between 0.85 and 0.92  $\mu\text{m}$ , owing to a crystal field effect. This feature falls within Landsat band 4, while a

reflectance high for all minerals is found in Landsat band 5 (Fig 9). This ratio will show higher values for oxidized iron rich rocks than for other types.

3- Band 5 / Band 7: The Al-OH and Mg-OH rotational effects associated with clays and other hydroxylated minerals result in absorption in Landsat band 7. When rationed against band 5, clay rich rocks show as bright areas (Fig. 10).

In the present study following ratio images: (5/7, 5/1, 4) and (5/7, 3/1, 4/3), in (R, G, and B) respectively were used for lithological discrimination of different rock types.

Thus the Cretaceous rocks are indicated by dark green color, the Eocene sediments are indicated by green to whitish green color the Oligocene rocks are indicated by orange color, the Pliocene sediments are indicated by whitish green color, the Miocene sediments are indicated by whitish blue color and Quaternary old terraces are indicated by yellowish color and the man made areas are purple color (Fig. 11).

Moreover, the ratio image (5/7, 3/1, 4/3 in R, G, B) were used also for more detailed lithological discrimination of different rock types.

The Cretaceous rocks are indicated by dark green color, the Eocene sediments are indicated by yellowish green color the Oligocene rocks are indicated by whitish green color, the Pliocene sediments are indicated by whitish yellow color, the Miocene sediments are indicated by purple color, Quaternary old terraces are indicated by pale green color and the old wadi deposits are indicated by whitish blue color and the man made areas are whitish green color (Fig. 12).

So, we used the Landsat ETM+ false color composite image bands (7, 4, 2) in RGB (Fig. 7) and the band ratios Landsat ETM+ images (Fig. 11) with the guidance of the geological map of EGSMA, scale of 1:100,000, to redraw the boundaries of the different rock units producing a new geological map of the study area.

ASTER data is characterized by a wide range of spectral bands (14 bands), which are excellent for lithologic discrimination. Based on spectral characteristic analysis (SCA) of the 3 VNIR and the 6 SWIR bands, two band-ratio images (1/5, 8/9, and 4/6) and (1/3, 2/5, and 4/9) in R, G, B were produced for better lithological discrimination (Hassan 2008).

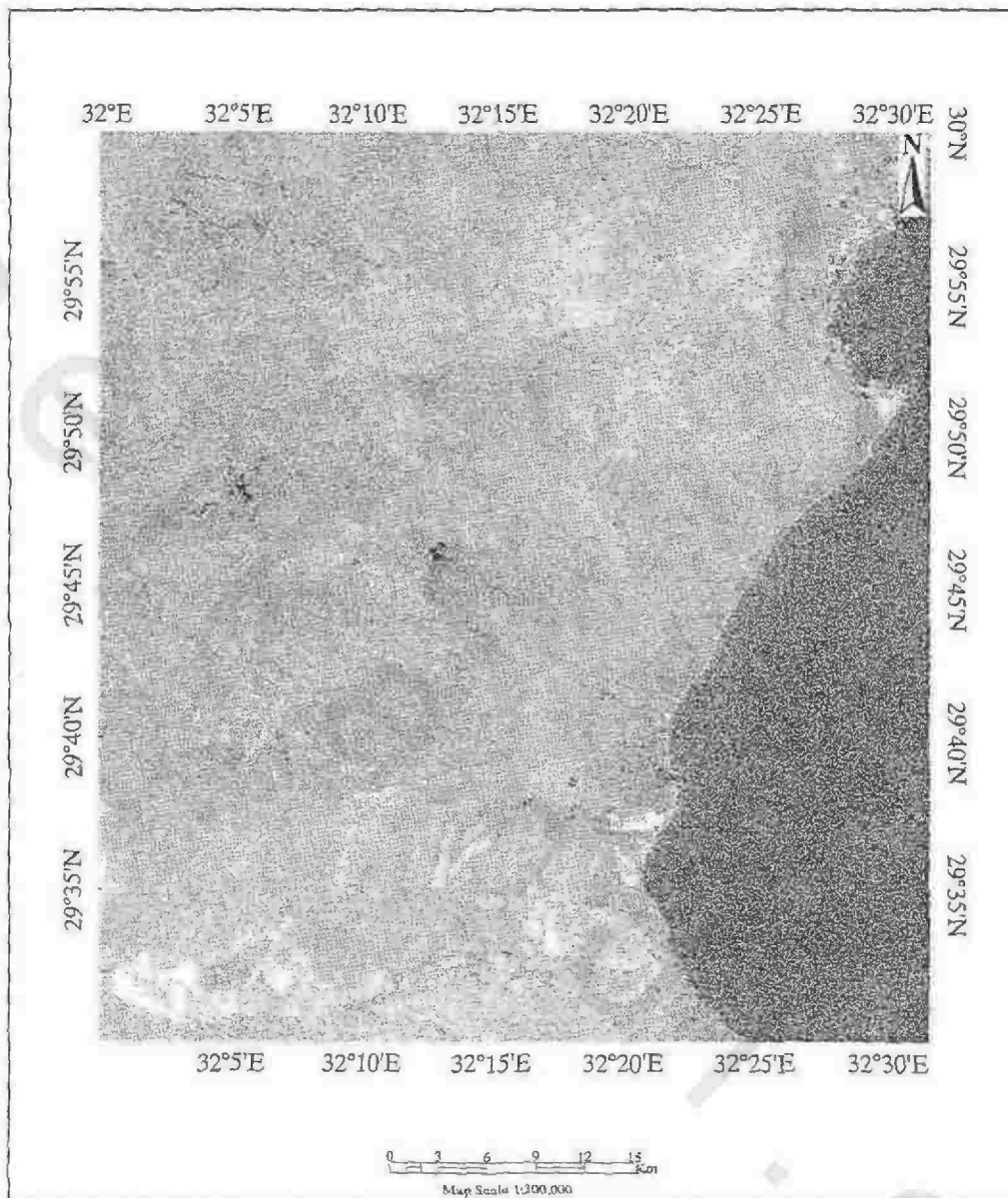


Figure (8): Landsat ETM+ ratio image (3/1) for the study area.

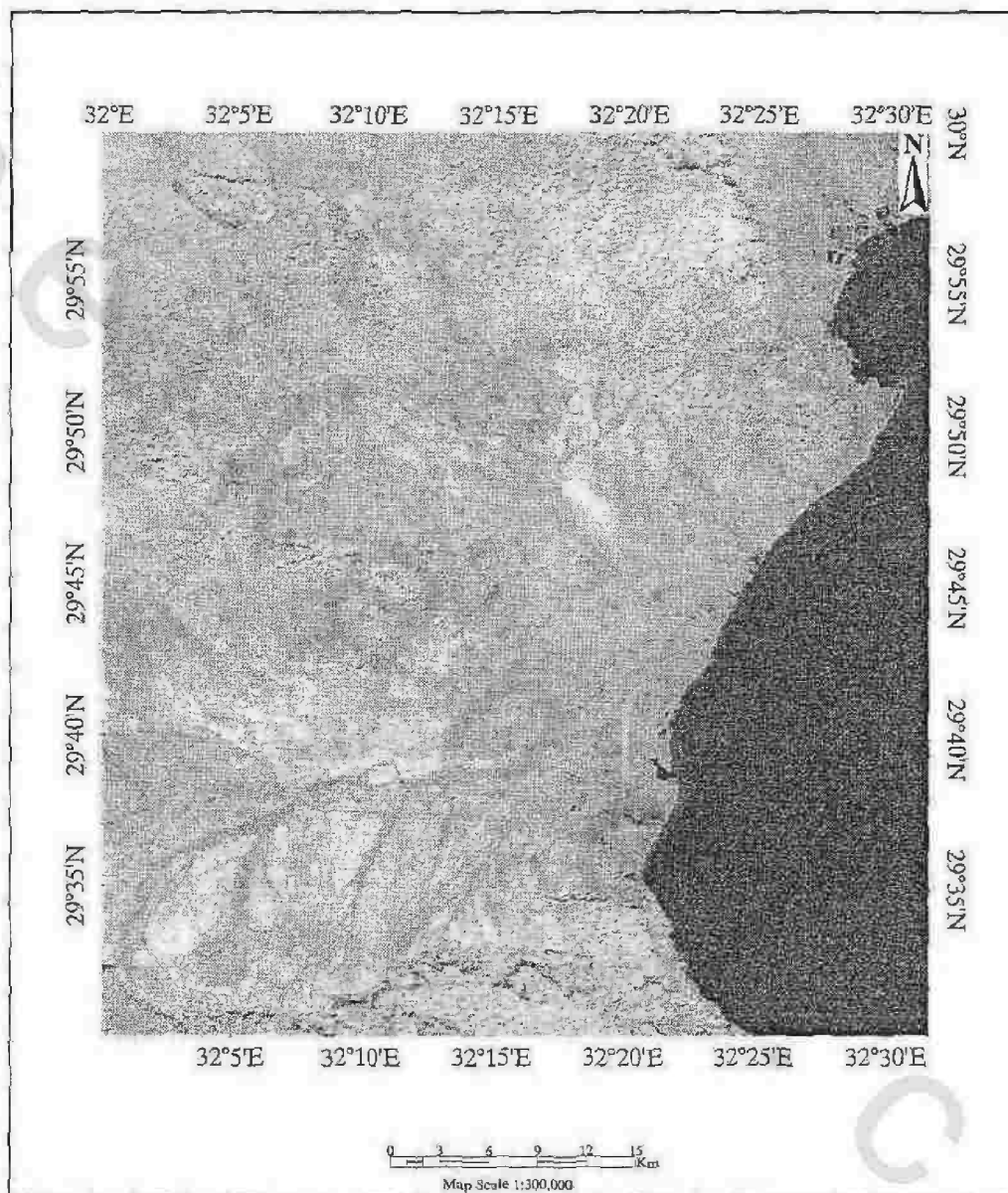


Figure (9): Landsat ETM+ ratio image (5/4) for the study area.

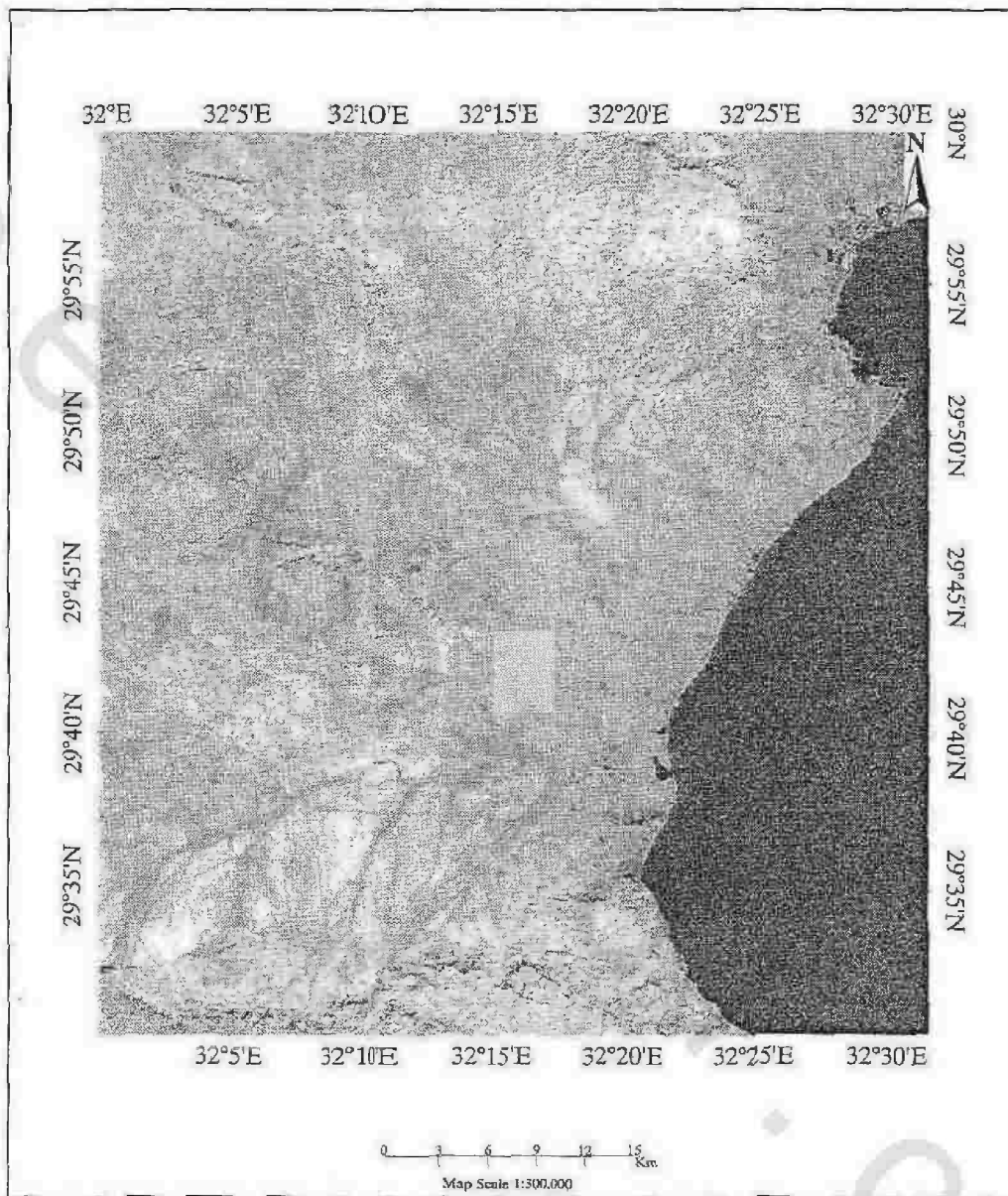


Figure (10): Landsat ETM+ ratio image (5/7) for the study area.

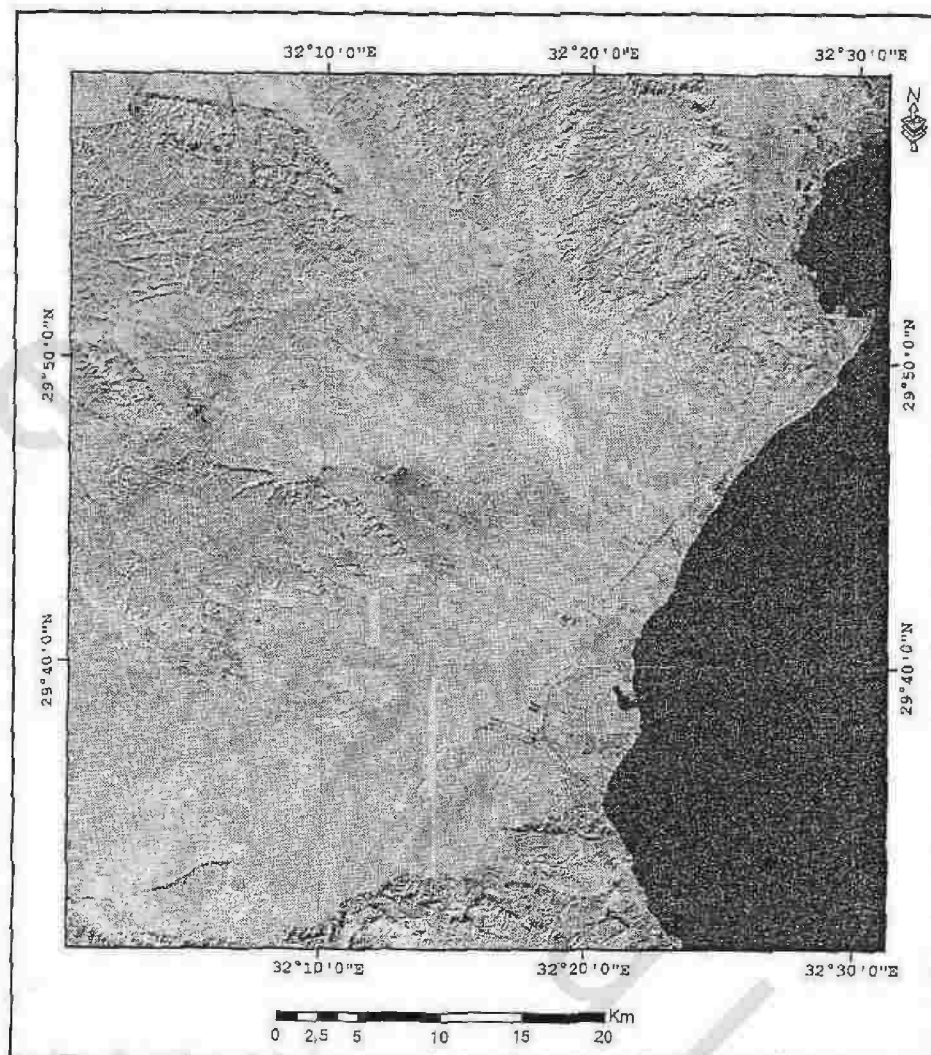


Figure (11): Landsat ETM+ ratio image (5/7, 5/1, 4) in RGB of the study area.

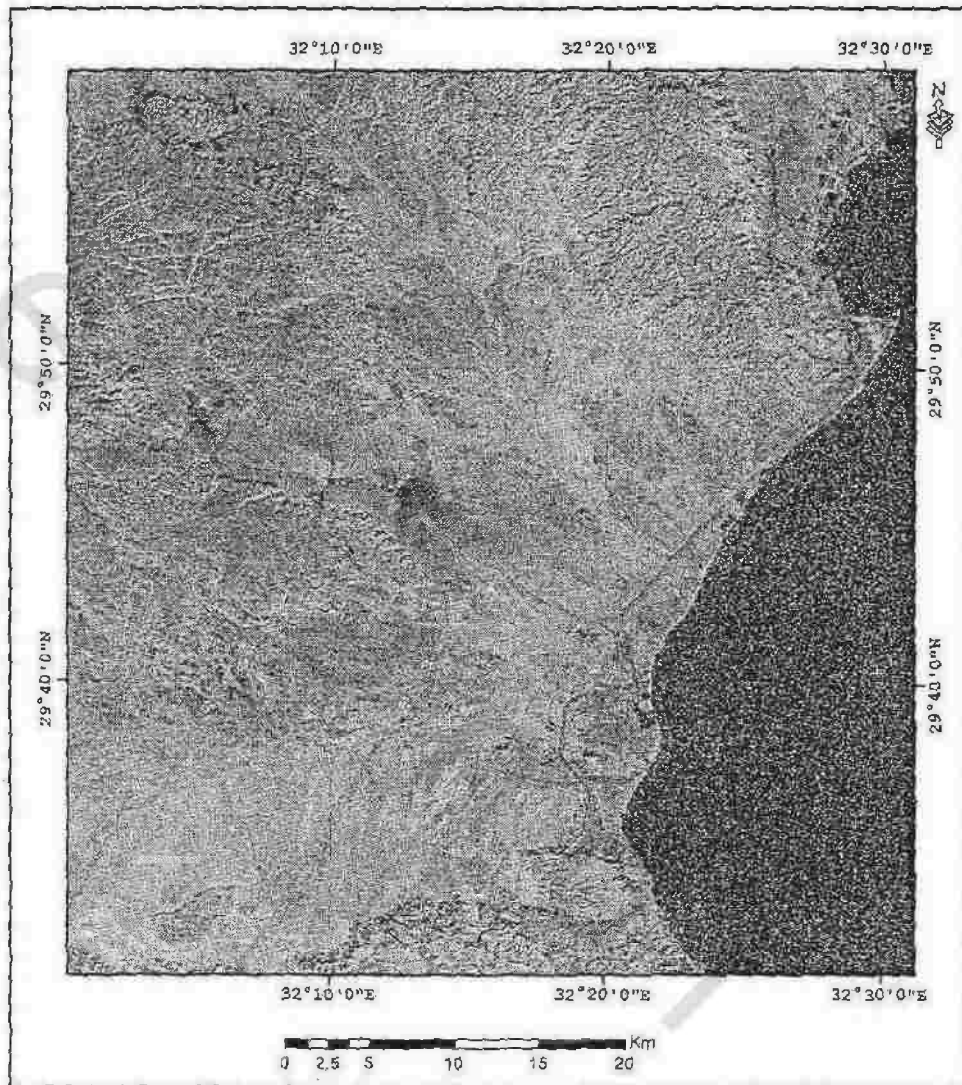


Figure (12): Landsat ETM+ ratio image (5/7, 3/1, 4/3) in RGB of the study area.

## II. 5. 6. Principle component analysis

The Principal Component (PC) Analysis process allowed the extraction of new information. It shows the directions of grey levels distribution in feature space. In general, PC analysis is a statistical technique widely used in RS to choose the suitable bands and to show spectral differences which helps to display clearly the correlation of the spectral values between the different channels. Due to the large number of spectral bands, much information was acquired from Landsat ETM+ images, especially in the infrared region of the spectrum. As result, these data were very useful for lithology, soil and terrain pattern differentiation.

Principle component analysis (PCA) is an attractive mean of incorporating spectral data from numerous dates into a small set of axes that contain most of the spectral information contained in the full multispectral, multitemporal data set (Eastman and Faulk, 1993; Richards, 1984).

Principle component analysis (PCA) is an image enhancement technique for displaying the maximum spectral contrast from (n) spectral bands with just three primary display colors. Principle component analysis (PCA) is often used as a method of data compression. In the present study, the pc transformation was computed for the study area to produce (pc1, pc2, pc3) in (RGB) respectively (Fig. 13) which comprises most of the various lithologic types. The computation processes were done using eight bands of the ETM+ data. The cretaceous has a greenish red color; the urban areas have deep yellow color. The Eocene rocks have pale violet color, while Miocene

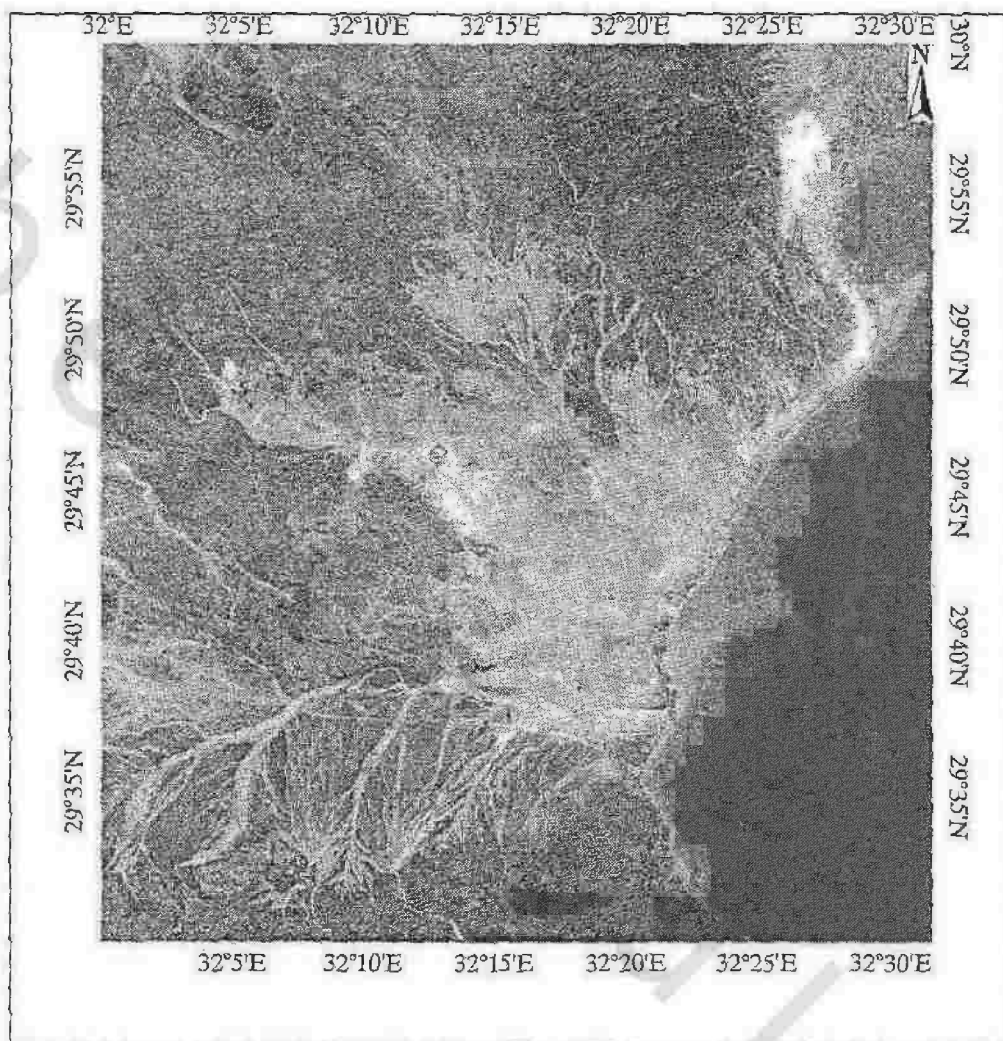


Figure ( 13 ): Principal component Landsat ETM+ image  
(pc1, pc2, Pc3) in RGB.

rocks pink and basalt deep red color. The Quaternary sandstone appears as violet and the wadies as yellow color.

### **II. 5. 7. Classification**

An important part of image analysis is identifying groups of pixels that have similar spectral characteristics and to determine the various features or land cover classes represented by these groups. Digital image classification is based on the spectral information used to create the image and classifies each individual pixel based on its spectral characteristics. The result of a classification is that all pixels in an image are assigned to particular classes or themes resulting in a classified image that is essentially a thematic map of the original image. The theme of the classification is selectable, thus a classification can be performed to observe land use patterns, geology, vegetation types, or rainfall. The objective of image classification is to match the spectral classes in the data to the information classes of our interest; where the spectral classes are groups of pixels that have nearly uniform spectral characteristic, but the information classes are the various themes or groups the user is attempting to identify in an image. Two methods of classification are commonly used: Unsupervised and Supervised.

Supervised classification requires the interpreter knows beforehand what classes are present and where each is in one or more locations within the scene. This cognition depends on the familiarity of user with the study scenes such as, user experience with the region, thematic maps, or by on-site visits. This familiarity allows the specialist to choose and set up discrete classes (Training sites) and the,

assign them category names. The automatic classification algorithm then extracts a spectral signature from each of the training sets and proceeds to automatically compare the spectral properties of every pixel in the image with the spectral signature of each target class. In which every pixel is compared with the various signature and assigned to the class whose signature comes closest. A few pixels in a scene do not match and remain unclassified, because these may belong to a class not recognized or defined. Supervised classification map, (Fig.14).

Unsupervised classification is done automatically by computer. In which, any individual pixel in the image of study area are examined automatically by compared to each discrete cluster to see which one it closest to and then classified into spectral classes. The grouping is based solely on the numerical information in the data and the spectral classes. In order to create an unsupervised classification the user typically determines the number of spectral classes to identify and a computer algorithm will find pixels with similar spectral properties and group them accordingly. Unsupervised classification map, (Fig. 15). Shows a specified 12 distinct of spectral classes in the study area, each of which is assigned by a color tone value.

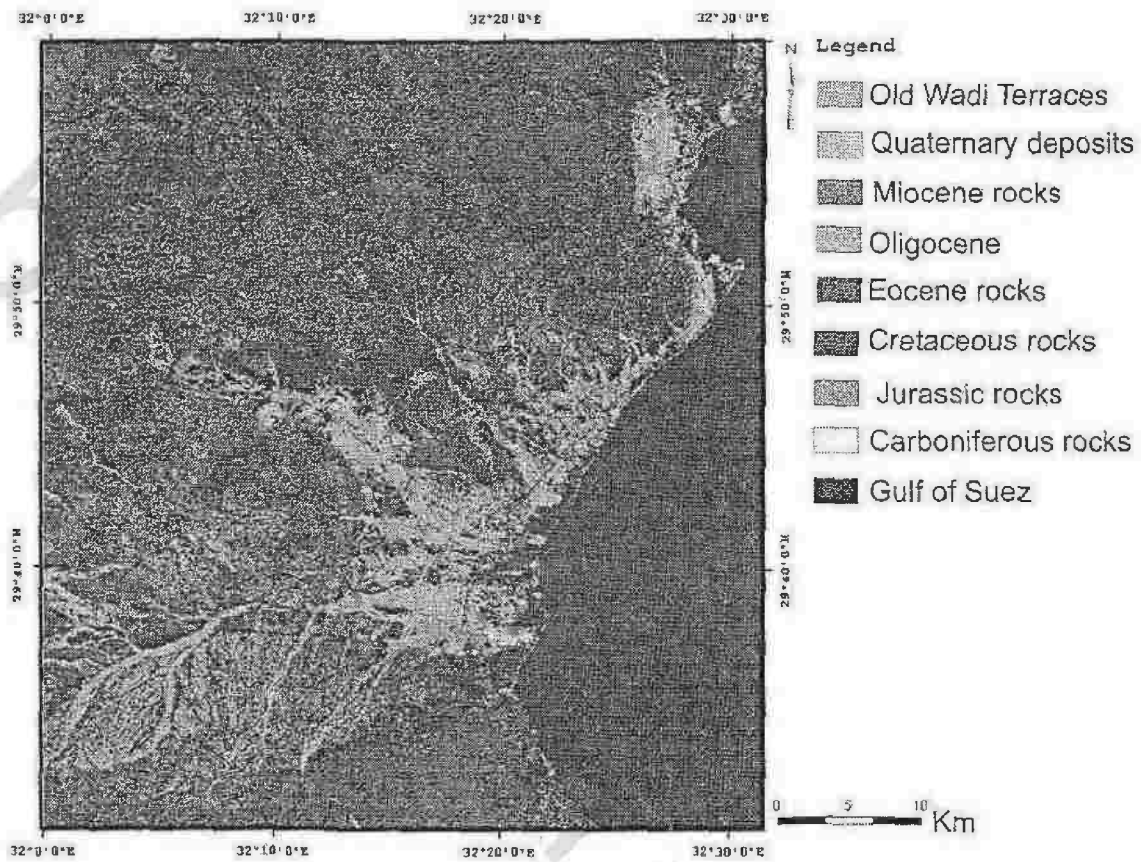


Figure (14): Landsat ETM+ image supervised classification.

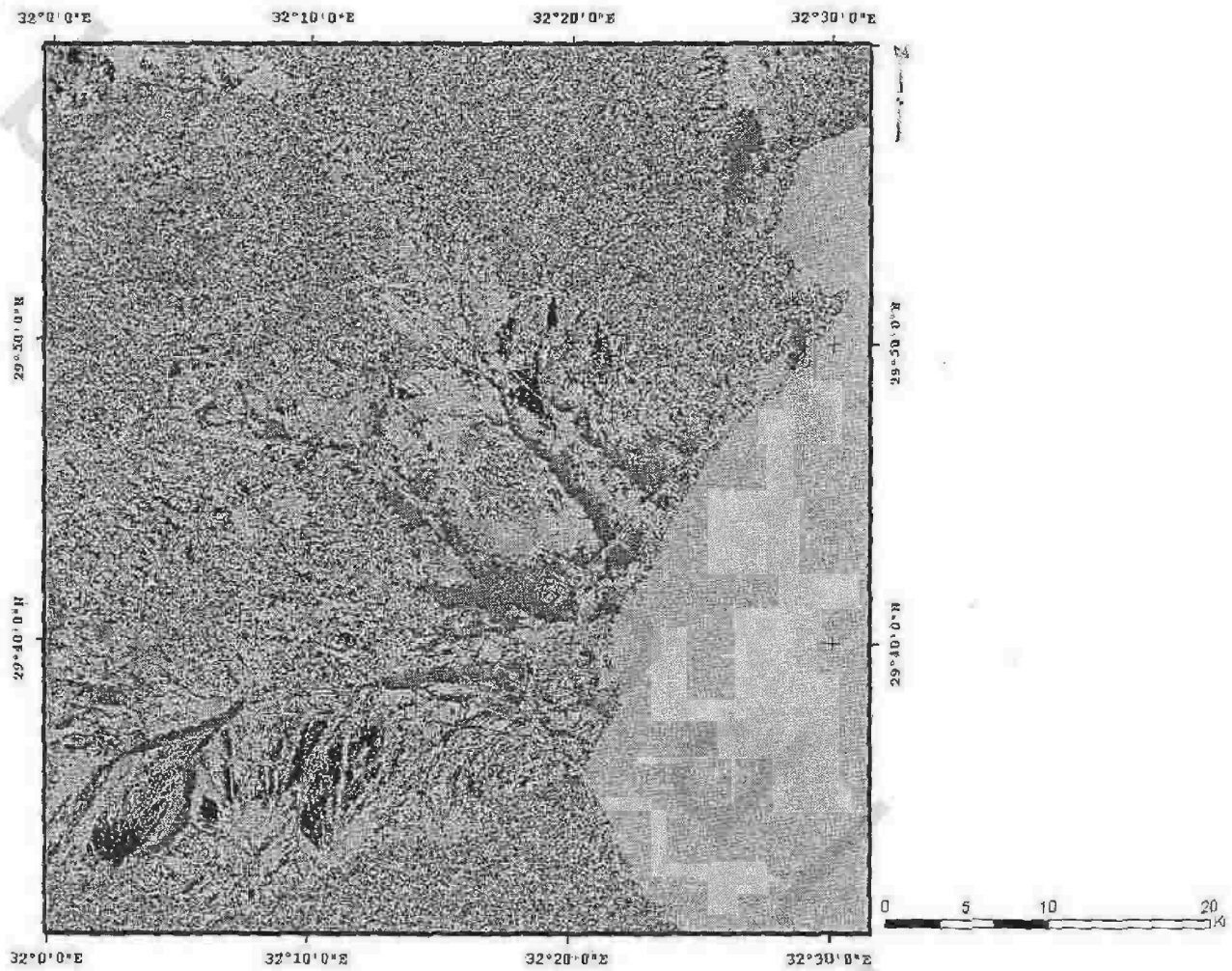


Figure (15): Landsat ETM+ image unsupervised classification.